


Article

Influence of Different pH Values on Gels Produced from Tea Polyphenols and Low Acyl Gellan Gum

Fangyan Zhang ^{1,2} , Xiangcun Wang ¹, Na Guo ^{1,2}, Huanhuan Dai ^{1,2}, Yimei Wang ¹, Yiwei Sun ¹ and Guilanzhu ^{1,2,*}

¹ Department of Biological and Food Engineering, Hefei Normal University, Lian Hua Road, Hefei 230601, China

² Anhui Engineering Laboratory for Medicinal and Food Homologous Natural Resources Exploration, Hefei 230601, China

* Correspondence: guilanz@hfnu.edu.cn

Abstract: To explore the influence of pH values on the properties of a compound system containing tea polyphenols (TPs) and low acyl gellan gum (LGG), the color, texture characteristics, rheological properties, water holding capacity (WHC), and microstructure of the compound system were measured. The results showed that the pH value noticeably affects the color and WHC of compound gels. Gels from pH 3 to 5 were yellow, gels from pH 6 to 7 were light brown, and gels from pH 8 to 9 were dark brown. The hardness decreased and the springiness increased with an increase in pH. The steady shear results showed that the viscosity of the compound gel solutions with different pH values decreased with increasing shear rates, indicating that all of the compound gel solutions were pseudoplastic fluids. The dynamic frequency results showed that the G' and G'' of the compound gel solutions gradually decreased with increasing pH and that G' was higher than G'' . No phase transition occurred in the gel state under heating or cooling conditions at pH 3, indicating that the pH 3 compound gel solution was elastic. The WHC of the pH 3 compound gel was only 79.97% but the WHC of compound gels pH 6 and pH 7 was almost 100%. The network structure of the gels was dense and stable under acidic conditions. The electrostatic repulsion between the carboxyl groups was shielded by H^+ with increasing acidity. The three-dimensional network structure was easily formed by an increase in the interactions of the hydrogen bonds.

Keywords: tea polyphenols; low acyl gellan gum; pH



Citation: Zhang, F.; Wang, X.; Guo, N.; Dai, H.; Wang, Y.; Sun, Y.; Zhu, G. Influence of Different pH Values on Gels Produced from Tea Polyphenols and Low Acyl Gellan Gum. *Gels* **2023**, *9*, 368. <https://doi.org/10.3390/gels9050368>

Academic Editor: Charalampos Proestos

Received: 24 March 2023

Revised: 21 April 2023

Accepted: 24 April 2023

Published: 28 April 2023



Copyright: © 2023 by the authors. Licensee MDPI, Basel, Switzerland. This article is an open access article distributed under the terms and conditions of the Creative Commons Attribution (CC BY) license (<https://creativecommons.org/licenses/by/4.0/>).

1. Introduction

Tea polyphenols (TPs) are natural antioxidants that are the main active ingredients in tea. Considering their good antioxidant, antiaging, and anticancer [1–3] functions, TPs have been widely used as a therapeutic agent or food supplement. However, their poor absorption, easy decomposition, and low metabolic transformation under physiological conditions limit their active functions [4]. TPs are sensitive to light, temperature, and pH, which makes them very unstable and easily oxidized [5–7]. To increase the effective use of TPs, several drawbacks must be overcome, such as oxidation and instability. Polyphenols and polysaccharides can form complexes through intermolecular interactions. In addition, the combination of TPs with hydrophilic polysaccharides can effectively prevent the oxidation process of TPs and improve their bioavailability [8].

Gellan gum (GG) is an anionic linear exopolysaccharide produced by the fermentation of *Sphingomonas paucimobilis*. It is a widely used microbial polysaccharide after xanthan gum. Its main chain is composed of 2 molecules of D-glucose, 1 molecule of D-glucuronic acid, and 1 molecule of L-rhamnose [9] in a 2:1:1 ratio linked together to form the linear primary structure [D-Glc(β1→4)D-GlcA(β1→4)D-Glc(β1→4)L-Rha(α1→3)]_n [10]. The structure of GG is shown in Figure 1.

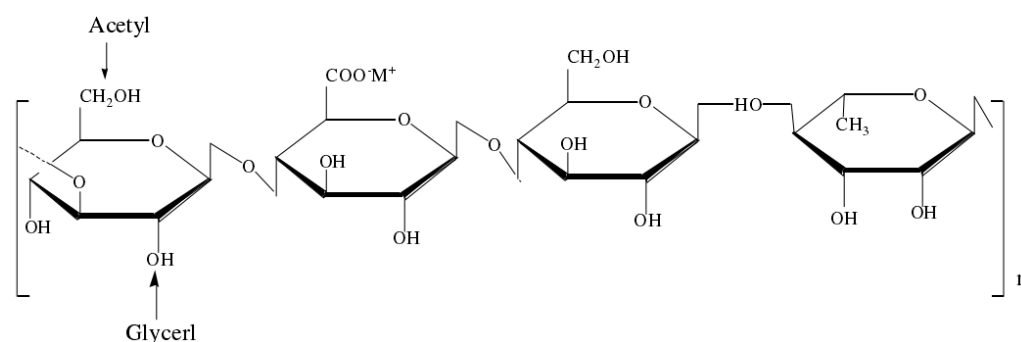


Figure 1. Structure of gellan gum.

Compared with plant gels, such as agar, gelatin, and pectin, and microbial gels, such as xanthan gum and pullulan, GG has certain advantages such as easy gel formation, high colloidal transparency, and resistance to enzymatic hydrolysis. It is mainly used as a gelling agent, stabilizer, suspending agent, and film-forming agent [11,12]. GG is mainly classified as a high acyl GG (HGG) or low acyl GG (LGG) and LGG is more widely used in the food industry [13,14]. Because the molecular structure of HGG is rich in acyl groups, it can form an elastic and tough opaque gel, while LGG can form a harder and more brittle transparent gel [15]. However, LGG is more susceptible to pH than HGG [16]. Therefore, our experiment selected LGG as our study material. TPs are rich in phenolic hydroxyl groups and can form hydrogen bonds with GG molecules to improve the viscosity and elasticity of the gel compound. The rich carboxyl and acyl groups in the molecular structure of GG also have a good compounding effect with TPs, which can delay the oxidation process of TPs and play a role in stabilization and slow release [17].

pH mainly affects the charge of biomacromolecules in gel molecules and the interactions between polymers. The binding ability of TPs to oat- β -glucan was the strongest at pH 6.0 [18]. pH was the most important factor that affected the interaction between cellulose and cyanidin-3-glucoside, and the binding ability of cyanidin-3-glucoside and cellulose varies with pH (3.0–5.0); the binding capacity of the two decreased when the pH increased to 7.0, which may be caused by the chemical structure of anthocyanins changing with pH [19]. pH (2.0–4.5) can also significantly affect the interaction between anthocyanins and pectics; the binding effect of the two is the strongest at pH 3.6 and the affinity between the two is relatively weak at other pH values [20]. Therefore, pH affects the properties of the compound gel formed by TPs and LGG.

In order to explore the effect of different pH values on the gel properties of the compound gels formed by TPs and LGG, we tested the color, texture characteristics, rheological properties, WHC, and microstructure of the compound gels with TPA, SEM, and FTIR. The results will provide a theoretical basis for the application of compound gels produced by TPs and LGG in real food systems and effectively improve the nutritional and functional properties of food.

2. Results and Discussion

2.1. Surface Color Analysis

We first examined the influence of pH on the color of compound gels because color measurements could enable us to distinguish the effect of pH on the TP-LGG compound gels. The color changes of the compound gels under different pH conditions are shown in Table 1 and Figure 2.

Table 1 shows that the L^* , a^* , and ΔE values increased, whereas the b^* values decreased with increased pH. The higher the L^* value is, the lighter the gel is [21,22]. The indicators L^* , a^* , b^* , and ΔE were positive values, indicating that the compound gels gradually changed from yellow to dark brown with increased pH. This was consistent with the observations in Figure 2. TPs were relatively stable under acidic conditions whereas they were very

unstable in neutral and alkaline solutions and decomposed in a few minutes [6], which caused the color of the compound gels to darken.

Table 1. Color change of the TP-LGG compound gels with pH 3–9.

pH	L^*	a^*	b^*	ΔE
3	12.28 ± 0.58^b	2.36 ± 0.09^b	10.55 ± 1.73^{ab}	28.27 ± 0.08^b
4	13.97 ± 0.90^{ab}	2.35 ± 0.18^b	11.89 ± 1.92^a	28.56 ± 1.40^b
5	13.95 ± 0.48^{ab}	2.82 ± 0.84^{ab}	11.32 ± 2.73^{ab}	28.74 ± 0.26^b
6	14.94 ± 0.58^a	2.41 ± 0.49^b	11.61 ± 1.77^a	28.02 ± 1.41^b
7	14.68 ± 0.94^a	3.48 ± 0.21^a	8.95 ± 0.32^{ab}	28.59 ± 0.35^b
8	13.20 ± 1.39^{ab}	2.86 ± 0.29^{ab}	7.33 ± 0.40^{bc}	30.74 ± 0.87^a
9	14.88 ± 0.88^a	2.96 ± 0.06^{ab}	5.33 ± 0.95^c	31.01 ± 0.17^a

The abc labeling method in statistics is a commonly used labeling method used to represent the significance and difference of statistical results. The difference between groups with the same letter is not significant, while the difference between groups with different letters is significant.

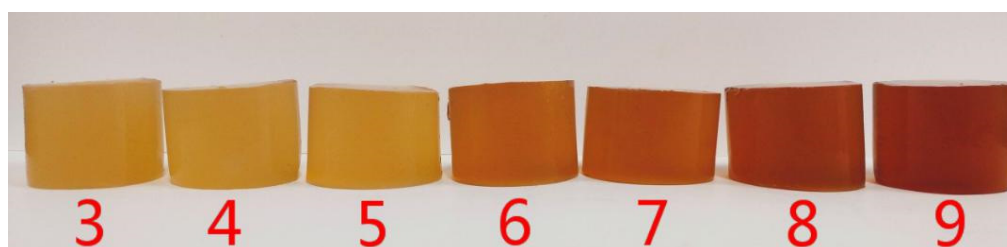


Figure 2. Color change of TP-LGG compound gels with different pH values. (number 3–9 mean pH values).

In the pH range of 3–5, the b^* value of the samples changed, and the color of the compound gels was yellow. However, when the pH was over 6, the b^* value decreased with increased pH. The compound gels became darker, considering that TPs are easily oxidized under alkaline conditions. At the same time, the difference in ΔE approached 3, indicating that the change in pH resulted in a visible change in the color of the compound gels.

The LGG gel was colorless and transparent. However, when TPs were added to LGG, the compound gels became yellow because of the presence of flavonoids and anthocyanins in the TPs. The natural pH of the TP-LGG gel was 5.2, and the compound gel was pale yellow. In the pH range of 3–5, the compound gels were still yellow. At pH 6–7, the compound gels were light brown. At pH 8–9, the compound gels were dark brown. This color change was expected because with the a^* value increased and the b^* value decreased, the red was deepened and the yellow was weakened so that the color of the compound gels changed as shown in Figure 2. TP solutions are oxidized into quinones mainly through oxidation and dimer formation, which deepened the color of the compound gels. The TP solution degraded irreversibly to a yellowish-brown solution due to the deterioration products, and this result was consistent with previous findings [23].

2.2. TPA Results

According to Figure 3, both the hardness and springiness of the compound gels with different pH values were significantly affected. The hardness decreased and the springiness increased as the pH rose from 3 to 9. The hardness of the compound gel (pH 3) reached a maximum value of 4216.377 g. Then, as the pH increased to 6, the hardness decreased abruptly. When the pH rose from 6 to 9, the hardness decreased slowly. This was consistent with previous findings that reported that hydrochloric acid acidifies LGG to make acid-sensitive colloids and found that the hardness and strength of the gel increased significantly when the pH decreased from 5 to 3 [24]. As the acidity of the compound gels continued to decrease, the concentration of H^+ in the system continued to increase. This shielded the negatively charged carboxyl groups in the molecular structure of GG, reduced the mutual

repulsion between polymers, and facilitated the formation of a three-dimensional network structure, thus enhancing the hardness of the compounded gel. The springiness of the gel was stable in the pH range of 6–9. However, the springiness of the compound gel was greatly weakened, and it became hard and brittle with the decrease in pH from 6 to 3, and reached a minimum at pH 3. Under weakly acidic conditions, the gel formed a dense three-dimensional network structure, making the gel more resistant to external impact. However, when the structure was completely destroyed, the network structure was more difficult to restore, making the gel less elastic.

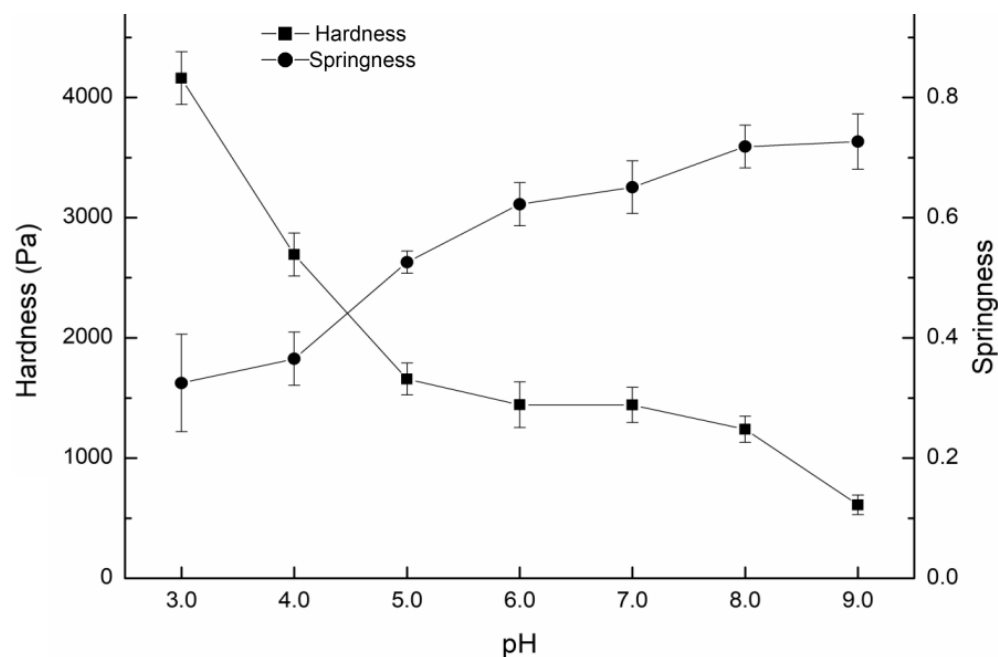


Figure 3. Hardness and springiness of the compound gels with different pH values.

2.3. Rheological Analyses

2.3.1. Steady Shear Analyses

During the stirring shear process, the molecular chains of TPLGG were straightened or dispersed under external forces, leading to an increase in the fluidity of the systems and a decrease in viscosity. This phenomenon is shear thinning and is commonly used to indicate the shear stability of systems during the shear process. The viscosity and shear stress of the TP-LGG compound systems is shown in Figure 4. As shown in Figure 4, the systems exhibited high viscosity at low shear rates, followed by a linear decrease in viscosity with the increasing shear rate, exhibiting a typical shear thinning behavior and indicating that the TP-LGG compound gel solutions were non-Newtonian fluids. The shear thinning behavior between TPs and LGG was mainly attributed to the destruction of intramolecular or intermolecular interactions [25,26] which caused a decrease in intermolecular electrostatic repulsion and an increase in mutual aggregation. At the same shear rate, the viscosity decreased as the pH increased from 3 to 9, and the viscosity of the compound gel solution was the highest at pH 3. H^+ could enhance the electrostatic repulsion between the negatively charged carboxyl groups in the LGG molecule under strongly acidic conditions, which made it easier to form a three-dimensional network structure in the gel solution. Strong interaction forces, such as hydrogen bonds between molecules, increased the viscosity of the compound gel solutions. The result was similar to the result of Picone and Cunha [27] who found that the viscosity of the gel increased when the pH of the LGG system was reduced from 5.3 to 3.5.

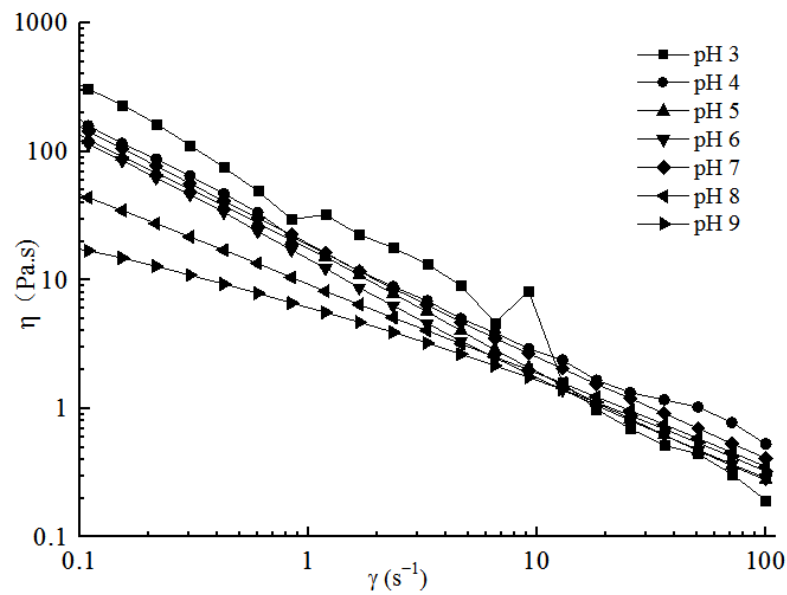


Figure 4. Variation in the viscosity of the gel solutions with different pH values.

2.3.2. Dynamic Frequency Sweep Analyses

As shown in Figure 5, the viscoelastic G' and G'' values of the compound gel solutions increased as the frequency rose from 0.01 to 6.105 Hz. The values of G' and G'' decreased with the increase in pH from 3 to 9. In the range of pH 3–7, G' was clearly higher than G'' , especially in the gel solutions of pH 3 and pH 4. The compound gel solutions were obviously predominantly elastic. The high concentration of H^+ in the system was conducive to the formation of a three-dimensional network structure, thereby enhancing the viscosity of the compound gel solutions. The G' and G'' of the compound gel solutions at pH 8 and pH 9 were raised but the G'' were higher than G' with low frequencies, and then G' were still higher than G'' later. Therefore, the compound gel solutions mainly exhibited solid-like characteristics from pH 3 to 9. Chen et al. [28] also found that LGG exhibited solid properties under acidic conditions, which was consistent with the results of this experiment.

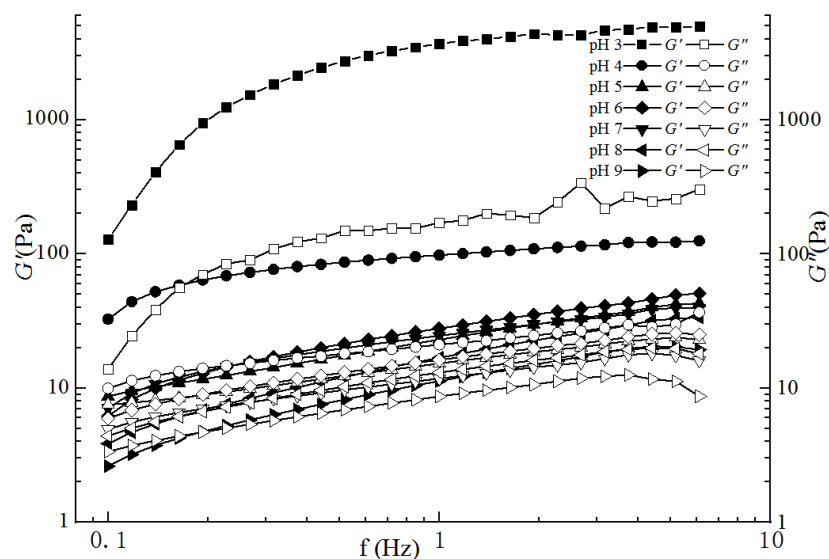


Figure 5. Frequency dependence of the compound gel solutions with different pH values.

2.3.3. Dynamic Temperature Scanning

As shown in Figure 6, whether in the process of heating or cooling, the G' and G'' of all samples generally decreased with the increase in pH value, and the G' and G'' of the pH 3 gel solution were the highest. During the heating process, except for the pH 3 gel solution, the G' and G'' values of the other compound gels decreased and underwent a solid-to-liquid transition. As shown in Figure 6a, the increase in pH value reduced the melting temperature of the gels. During the cooling process, the G' and G'' values of all the compound gels increased, and some gels underwent a liquid-to-solid transition. As shown in Figure 6b, the pH value has an effect on the freezing point of the compound gel during the cooling process. In comparison with the dynamic temperature scan curves under the two conditions, the gelling temperature under cooling conditions was lower than the melting temperature under heating conditions, and an obvious hysteresis phenomenon occurred. The compound gel solution at pH 3 had no phase transition and occurred in the gel state under both heating and cooling conditions, indicating that the pH 3 compound gel solution was elastic. Similar to the findings of Li et al. [11], who used glucono- δ -lactone to prepare thermally irreversible gels of LGG, decreasing pH is usually more effective in promoting gellan gelation.

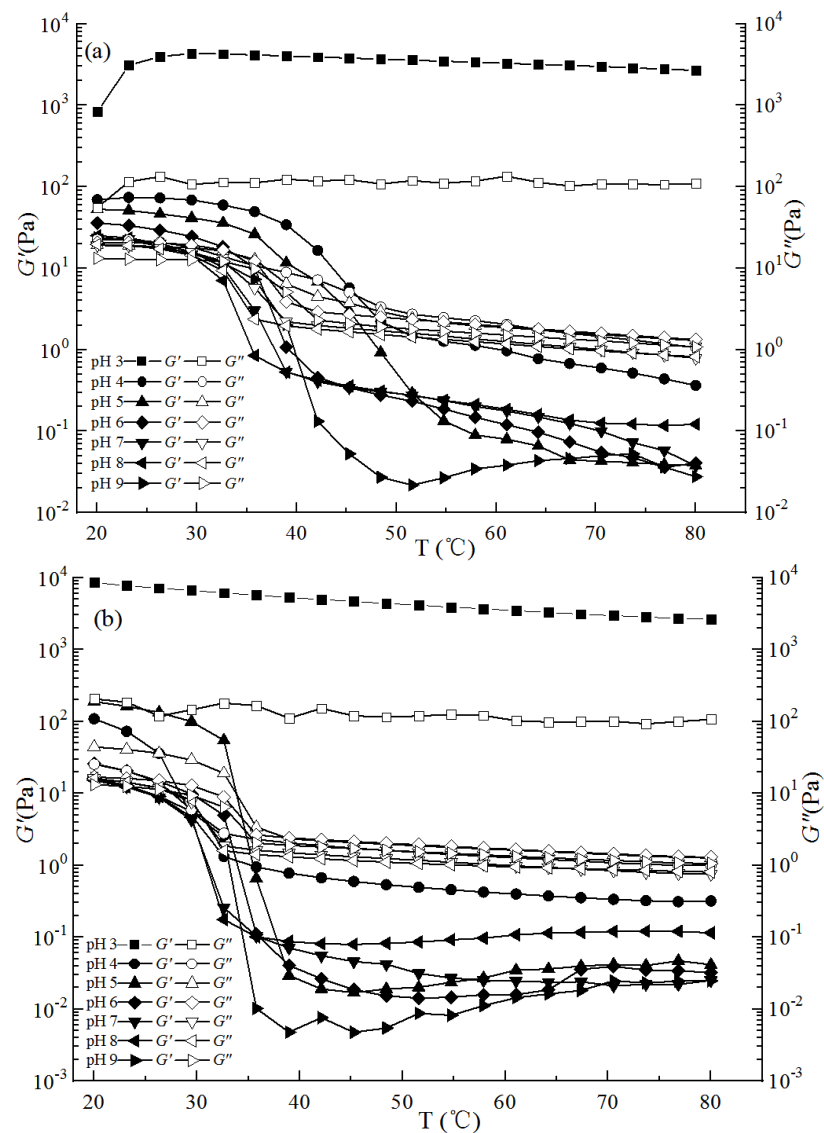


Figure 6. Effects of heating and cooling frequency on the G' and G'' of the compound gel solutions with different pH values ((a) indicates the heating process; (b) indicates the cooling process).

2.4. WHC

The WHC of the compound gels with different pH values is shown in Figure 7. The WHC of the compound gels increased from pH values 3 to 6 and reached a maximum at pH 6. Interestingly, the WHC of the pH 6 compound gel was the same as that of the pH 7 compound gel, which is almost 100%. Then, the WHC of the compound gels began to decrease as the pH value increased from 7 to 9. The results showed that the WHC of the compound gels was relatively stable at pH 6–8. When the acidity was reduced to pH 5, the WHC of the gels started to decrease and was the lowest at pH 3, only 79.97%. The dissociation degree of the carboxyl group of the hydrophilic group in LGG decreased under acidic conditions. Consequently, the WHC of the gel decreased. The decrease in the WHC of the pH 9 compound gel can be attributed to the decreased hydrophilic groups such as hydroxyl groups caused by the oxidation of TPs, thus reducing the WHC of the compound gels. Previous studies suggested that the WHC was significantly reduced under the acidic condition of LGG [28].

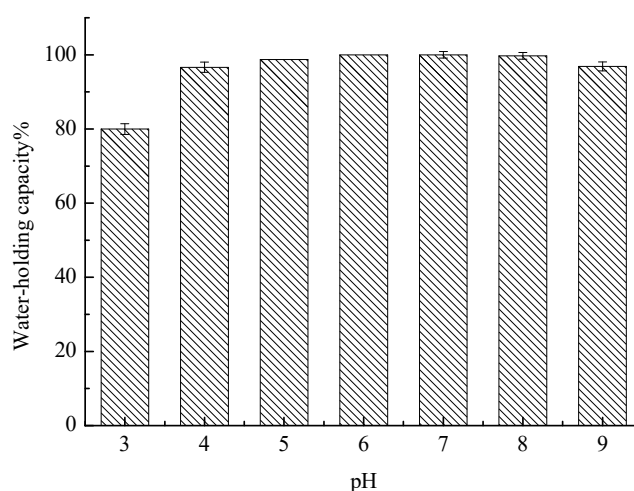


Figure 7. Effect of pH on the WHC of the compound gels.

2.5. Microstructure Analysis

The SEM images revealed that pH affected the morphology of the compound gel system as seen in Figure 8. The microstructure of the compound gel at pH 3 (Figure 8a) was heterogeneous and porous, with numerous “water channels” inside the gel structure. H^+ reduced the degree of dissociation of carboxyl groups and shielded the electrostatic repulsion between the carboxyl groups to promote the formation of a double helix structure which was conducive to the formation of a compact three-dimensional network structure [28]. Therefore, the WHC of the pH 3 gel was the weakest. However, the gel microstructure became more inhomogeneous as the pH increased. When the pH was 7 (Figure 8b), the internal structure of the compound gel was relatively stable, improving the WHC of the gel. At pH 9 (Figure 8c), the network structure formed in the internal structure of the compound gel was relatively disordered. Considering that the electrostatic repulsion between the carboxyl groups in LGG molecules was strong under alkaline conditions and that the double helix between polymers was degraded, the formation of a network structure was not induced. Meanwhile, TPs were oxidized and their interaction with LGG molecules was affected, resulting in the chaotic internal structure of the compound gels. The network structure of the LGG was weak under alkaline conditions according to electron microscope scanning [29]. Microscopy images showed that the pH had obvious effects on the microstructure of the compound gels.

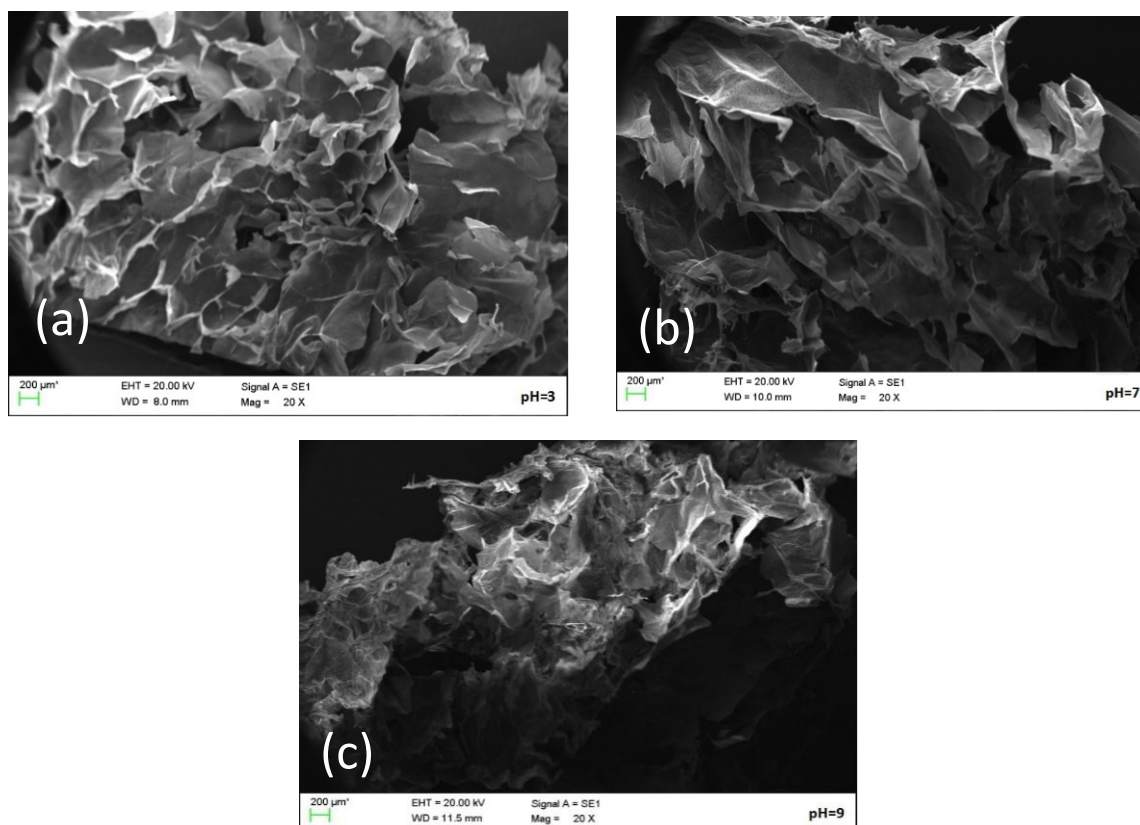


Figure 8. SEM images of compound gels with different pH values. ((a) means the compound gel with pH 3; (b) means the compound gel with pH 7; (c) means the compound gel with pH 9).

2.6. FTIR Spectra Analysis

FTIR analysis was performed to confirm the cross-linking interactions between TPs and LGG. The infrared absorption spectra of the compound gels with different pH values are shown in Figure 9. The compound gels with different pH values had similar absorption peak shapes with slightly different intensities and positions. Although the sample was freeze-dried and still contained bound water, the wide absorption peak in the range of $3500\text{--}3100\text{ cm}^{-1}$ was mainly the superposition of the O–H stretching vibration and water in the gels. The stretching vibration of O–H near 3314.07 cm^{-1} included inter- and intra-molecular interactions [29]. The hydroxyl groups of samples existed in an associative manner so the absorption peak was very wide. Under acidic conditions, more hydrogen bonds were generated between water molecules and between them and other components, resulting in an increase in the intensity of the O–H absorption peak [30]. A strong absorption near 1602.56 cm^{-1} could be attributed to the C–O stretching vibrations in the LGG molecule. A weak absorption near 1411.16 cm^{-1} could be attributed to the O–H bending vibration. The absorption peak near 1028.15 cm^{-1} was associated with the stretching vibration of C–O–C. The spectra of compound gels showed characteristic peaks near 1602.56 cm^{-1} (C–O stretching vibrations), 1407.30 cm^{-1} (O–H bending vibration), and 1021 cm^{-1} (C–O–C stretching) [31]. Overall, the intensity of the absorption peak weakened and slightly moved towards the low-frequency direction as the pH value increased, indicating that with the increase in H^+ concentration, the dissociation degree of the carboxyl group was inhibited, and the electrostatic interaction between polymers decreased. Therefore, we speculated that the change in pH could not generate a new chemical bond between TPs and LGG. Based on the FTIR results, we concluded that TPs were compatible with LGG during the mixing and gelation stage due to intermolecular synergistic effects and hydrogen bonding [32].

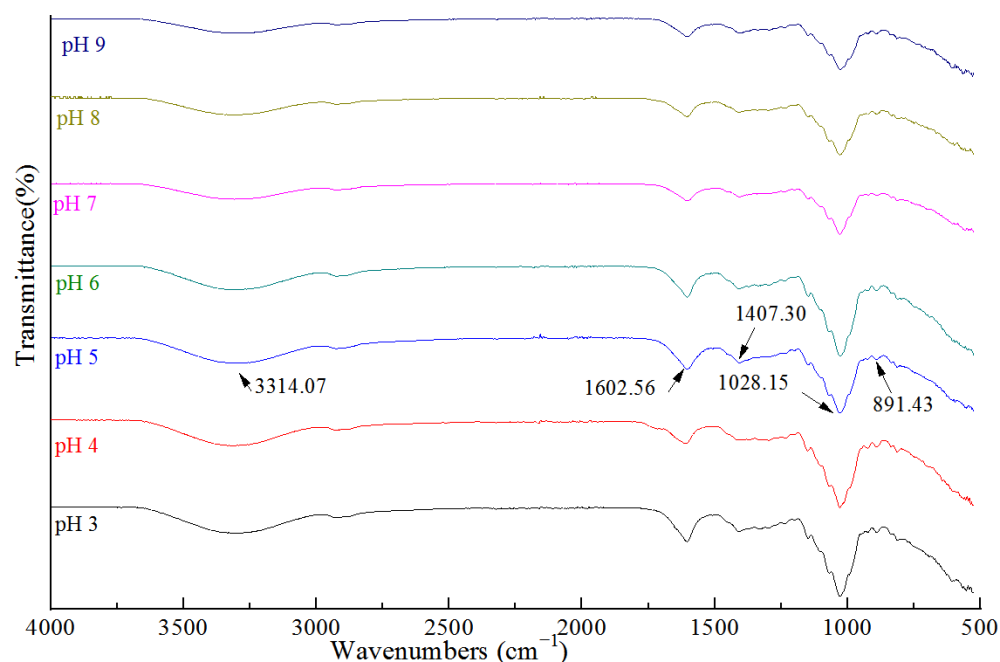


Figure 9. Fourier transform infrared spectra of the compound gels.

3. Conclusions

The results of this work showed that pH affected the properties of TP-LGG compound gels. The compound gels turned from yellow to brown and then to dark brown with increasing pH. In addition, the hardness of the compound gels rose, and the springiness decreased continuously with increasing pH. The steady shear results showed that the viscosity of the compound gel solutions with different pH values decreased with increasing shear rates, indicating that the compound gel solutions were pseudoplastic fluids. The compound gel solutions mainly exhibited solid-like characteristics in the acidic and neutral ranges and exhibited liquid-like properties under weakly alkaline conditions. The compound gels also underwent a solid-to-liquid transition in the process of heating and cooling. The values of G' and G'' decreased with increasing pH. The WHC of the gels was relatively stable and strong in the neutral and weakly alkaline ranges, but the WHC under acidic conditions was the weakest. Furthermore, the network structure of the compound gels was relatively dense and stable under acidic conditions and, finally, there were cross-linking reactions between TPs and LGG with increasing acidity.

4. Materials and Methods

4.1. Materials

LGG (food grade) was obtained from the Ruifeng (Henan, China). TPs (food grade) were obtained from the Naman (Nanjing, China). Hydrochloric acid and sodium hydroxide were obtained from Meifeng (Hefei, China).

4.2. Preparation of TP-LGG Compound Gels

A 1.0% (*w/w*) LGG solution and 0.15% (*w/w*) TP solution were prepared by dissolving them in deionized water and stirring at 90 °C to ensure complete powder hydration and dissolution. The pH of the system was adjusted to 3, 4, 5, 6, 7, 8, and 9 with 1.0 M NaOH or 1.0 M HCl solution. A pH meter (FE20K, Mettler Toledo, Leicester, UK) was used to measure the pH of the solution. Then, 0.15 mL of 2 M Ca^{2+} solution was added to the compound gel. Finally, the compound gel was placed in a plastic casing while it was still hot and stored in a refrigerator at 4 °C for 24 h after cooling.

4.3. Color Measurements

The color was measured as previously described [33,34], with some modifications. A colorimeter (CR-400, Konica Minolta, Tokyo, Japan) was used to observe the color changes of the gels. The color was denoted by the a , b , and L values, indicating redness/greenness, yellowness/blueness, and lightness, respectively. The machine was calibrated using a standard white tile, and the L^* , a^* , and b^* values were obtained. The total color difference (ΔE) was calculated using the following equation:

$$\Delta E = \sqrt{(\Delta L^*)^2 + (\Delta a^*)^2 + (\Delta b^*)^2}$$

4.4. Texture Profile Analysis (TPA) of TP-LGG Compound Gels

The gels were cut into cylinders with a height of 25 mm and radius of 25 mm, and the TA-XT plus (Stable Micro Systems, Surry, UK) physical property analyzer was used for measurements. The parameters of the tests were set as follows: measure type, TPA; probe type, P/50; compression strain, 50%; pretest speed, 5.0 mm/s; test speed, 1.0 mm/s; and post-test speed, 5.0 mm/s. Based on the characteristics of the samples, data on hardness (g) and springiness (g) were recorded and used as the analysis index [25].

4.5. Rheological Measurements of TP-LGG Compound Gels

4.5.1. Steady Shear Analyses

The steady rheology was tested as previously described [35,36], with some modifications. The rheological properties of the compound gel solutions were studied using a rheometer (HAAKE RS6000) with flat rotor model P35 TiL (diameter, 35 mm; gap, 1 mm). Samples were tested at 25 °C with steady shear rates in the range of 0.1–100 s⁻¹, and the viscosity of the compound gel solutions was recorded.

4.5.2. Dynamic Frequency Sweep Rheological Measurements

Frequency sweep measurements at a fixed amplitude of shear stress were carried out in the frequency range of 0.01–10 Hz at 25 ± 0.1 °C. The values of the storage modulus (G') and loss modulus (G'') were recorded [36].

4.5.3. Dynamic Temperature Sweep Rheological Measurements

Temperature sweeps were conducted at a heating rate of 5 °C/min, reduced from 80 °C to 20 °C, and finally increased from 20 °C to 80 °C, with a sweep frequency of 1 rad/s and shear stress of 5 s⁻¹. The G' and G'' values were recorded.

4.6. Water Holding Capacity (WHC)

The WHC was studied as follows: the gel was loaded into a 1.5 mL empty centrifuge tube and centrifuged at 10,000 × g for 30 min with an ultracentrifuge. Then, the water was removed, and the mass of the remaining gel was recorded [37].

$$WHC(\%) = \frac{m_2 - m_0}{m_1 - m_0} \times 100\%$$

where m_0 is the mass/g of the centrifuge tube, m_1 is the total mass/g of the gel and centrifuge tube before centrifugation, and m_2 is the total mass/g of the gel and centrifuge tube after centrifugation.

4.7. Scanning Electron Microscopy (SEM)

The surface morphology of the compound gels was visualized using a cold field emission SEM (EVOMA15, Carl Zeiss AG Co., Ltd., Oberkochen, Germany) operated at an accelerating voltage of 1 kV. Prior to detection, the gel samples, which were cut into thin slices with a diameter of 3 mm after freeze-drying, were fixed on copper stubs and sputtered with gold, and pictures were taken at 20× magnification.

4.8. Fourier Transform Infrared Spectroscopy (FTIR)

The chemical interactions between the TP functional groups and LGG were investigated using an FTIR spectrophotometer (Nicolet6700, Thermo Fisher Scientific, MA, USA) as previously described [38], with some modifications. The FTIR studies of the gels were carried out by using the KBr pellet method. After freeze-drying, the gel samples were pressed with KBr and then scanned using an FTIR spectrometer in the scanning range of 400–4000 cm^{-1} and a resolution of 4 cm^{-1} .

4.9. Statistical Analysis

All tests were conducted in a completely randomized design in independent triplicates to confirm the reproducibility of the results. The drawn figures in this article were processed using Origin Pro 8.0 (OriginLab Inc., Northampton, MA, USA). Duncan's multiple range test determined significant differences, at the 95% confidential level ($p < 0.05$), using statistical SPSS software.

Author Contributions: Conceptualization, N.G. and G.Z.; Data curation, N.G.; Formal analysis, F.Z. and X.W.; Investigation, H.D., Y.S. and Y.W.; Methodology, F.Z. and X.W.; Project administration, N.G. and G.Z.; Supervision, H.D.; Writing—original draft, F.Z.; Writing—review and editing, G.Z. All authors have read and agreed to the published version of the manuscript.

Funding: This research received funding supported by the Top-Notch Talents in Disciplines (Majors) of Colleges and Universities in Anhui Province (grant number gxbjZD2020082), Anhui Engineering Laboratory for Medicine and Food Homologous Natural Resources Exploration (grant number YSTY2022002, YSTY2022015, YSTY2022031), the Department of Education Natural Research Project of Anhui Provincial (2022AH052163, 2022AH052147, 2022AH040288, 2022AH052122, KJ2020A0115).

Institutional Review Board Statement: Not applicable.

Informed Consent Statement: Not applicable.

Data Availability Statement: Data are contained within the article.

Conflicts of Interest: The authors declare no conflict of interest.

References

1. Zhang, W.; Liu, Y.; Zhang, X.; Wu, Z.; Weng, P. Tea polyphenols-loaded nanocarriers: Preparation technology and biological function. *Biotechnol. Lett.* **2022**, *44*, 387–398. [[CrossRef](#)] [[PubMed](#)]
2. Yan, Z.; Zhong, Y.; Duan, Y.; Chen, Q.; Li, F. Antioxidant mechanism of tea polyphenols and its impact on health benefits. *Anim. Nutr.* **2020**, *6*, 115–123. [[CrossRef](#)] [[PubMed](#)]
3. Wang, S.-T.; Cui, W.-Q.; Pan, D.; Jiang, M.; Chang, B.; Sang, L.-X. Tea polyphenols and their chemopreventive and therapeutic effects on colorectal cancer. *World J. Gastroenterol.* **2020**, *26*, 562–597. [[CrossRef](#)] [[PubMed](#)]
4. Zaveri, N.T. Green tea and its polyphenolic catechins: Medicinal uses in cancer and noncancer applications. *Life Sci.* **2006**, *78*, 2073–2080. [[CrossRef](#)]
5. Sun, B.; Wang, W.; He, Z.; Zhang, M.; Kong, F.; Sain, M.; Ni, Y. Improvement of Stability of Tea Polyphenols: A Review. *Curr. Pharm. Des.* **2018**, *24*, 3410–3423. [[CrossRef](#)]
6. Zhu, Q.Y.; Zhang, A.; Tsang, D.; Huang, Y.; Chen, Z.-Y. Stability of Green Tea Catechins. *J. Agric. Food Chem.* **1997**, *45*, 4624–4628. [[CrossRef](#)]
7. Mochizuki, M.; Yamazaki, S.-I.; Kano, K.; Ikeda, T. Kinetic analysis and mechanistic aspects of autoxidation of catechins. *Biochim. Biophys. Acta (BBA)-Gen. Subj.* **2002**, *1569*, 35–44. [[CrossRef](#)]
8. Yi, J.J.; Zhao, Y.; Bi, J.; Lu, J.; Zhou, M. A review of interactions between cell wall polysaccharides and polyphenols in fruits and vegetables. *Food Sci.* **2020**, *41*, 269–275. [[CrossRef](#)]
9. O'Neill, M.A.; Selvendran, R.R.; Morris, V.J. Structure of the acidic extracellular gelling polysaccharide produced by *Pseudomonas elodea*. *Carbohydr. Res.* **1983**, *124*, 123–133. [[CrossRef](#)]
10. Gonçalves, V.M.; Reis, A.; Domingues, M.R.M.; Lopes-Da-Silva, J.A.; Fialho, A.M.; Moreira, L.M.; Sá-Correia, I.; Coimbra, M.A. Structural analysis of gellans produced by *Sphingomonas elodea* strains by electrospray tandem mass spectrometry. *Carbohydr. Polym.* **2008**, *77*, 10–19. [[CrossRef](#)]
11. Li, A.; Gong, T.; Li, X.; Li, X.; Yang, X.; Guo, Y. Preparation of thermally stable emulsion gels based on Glucono- δ -lactone induced gelation of gellan gum. *Int. J. Biol. Macromol.* **2020**, *156*, 565–575. [[CrossRef](#)]
12. Prajapati, V.D.; Jani, G.K.; Zala, B.S.; Khutliwala, T.A. An insight into the emerging exopolysaccharide gellan gum as a novel polymer. *Carbohydr. Polym.* **2013**, *93*, 670–678. [[CrossRef](#)]

13. Abramovič, H.; Klofutar, C. Water adsorption isotherms of some gellan gum samples. *J. Food Eng.* **2006**, *77*, 514–520. [[CrossRef](#)]
14. Chen, Q.; Li, R.; Zhou, T.; Cheng, H.; Han, X. Effect of preparation conditions on fluid gel formation of Gellan gum. *Food Sci.* **2020**, *41*, 23–29.
15. Bradbeer, J.F.; Hancocks, R.; Spyropoulos, F.; Norton, I.T. Low acyl gellan gum fluid gel formation and their subsequent response with acid to impact on satiety. *Food Hydrocoll.* **2015**, *43*, 501–509. [[CrossRef](#)]
16. Chen, Q.; Zhou, T.; Cheng, H.; Han, X. Gelation properties of low acyl and high acyl mixed acid gellan gels. *Trans. Chin. Soc. Agric. Mach.* **2020**, *51*, 360–365. [[CrossRef](#)]
17. Zhu, G.L.; Guo, N.; Ma, M.; Ning, Y.; Ni, Z.H. Study on the properties of gelatin-tea polyphenol compound film. *Food Ferment. Ind.* **2019**, *45*, 72–77. [[CrossRef](#)]
18. Wu, Z.; Li, H.; Ming, J.; Zhao, G. Optimization of Adsorption of Tea Polyphenols into Oat β -Glucan Using Response Surface Methodology. *J. Agric. Food Chem.* **2011**, *59*, 378–385. [[CrossRef](#)]
19. Phan, A.S.T.; Netzel, G.; Wang, D.; Flanagan, B.M.; D’Arcy, B.R.; Gidley, M.J. Binding of dietary polyphenols to cellulose: Structural and nutritional aspects. *Food Chem.* **2015**, *171*, 388–396. [[CrossRef](#)]
20. Lin, Z.; Fischer, J.; Wicker, L. Intermolecular binding of blueberry pectin-rich fractions and anthocyanin. *Food Chem.* **2016**, *194*, 986–993. [[CrossRef](#)]
21. Kim, E.; Liang, Y.; Jin, J.; Sun, Q.; Lu, J.; Du, Y.; Lin, C. Impact of heating on chemical compositions of green tea liquor. *Food Chem.* **2006**, *103*, 1263–1267. [[CrossRef](#)]
22. Zeng, L.; Ma, M.; Li, C.; Luo, L. Stability of tea polyphenols solution with different pH at different temperatures. *Int. J. Food Prop.* **2016**, *20*, 1–18. [[CrossRef](#)]
23. Shpigelman, A.; Israeli, G.; Livney, Y.D. Thermally-induced protein–polyphenol co-assemblies: Beta lactoglobulin-based nanocomplexes as protective nanovehicles for EGCG. *Food Hydrocoll.* **2010**, *24*, 735–743. [[CrossRef](#)]
24. Cassanelli, M.; Prosapio, V.; Norton, I.; Mills, T. Acidified/basified gellan gum gels: The role of the structure in drying/rehydration mechanisms. *Food Hydrocoll.* **2018**, *82*, 346–354. [[CrossRef](#)]
25. Wang, J.; Zhao, X.; Zhou, C.; Wang, C.; Zheng, Y.; Ye, K.; Li, C.; Zhou, G. Effects of gellan gum and inulin on mixed-gel properties and molecular structure of gelatin. *Food Sci. Nutr.* **2021**, *9*, 1336–1346. [[CrossRef](#)]
26. Grisel, M.; Muller, G. Rheological Properties of the Schizophyllan–Borax System. *Macromolecules* **1998**, *31*, 4277–4281. [[CrossRef](#)]
27. Picone, C.S.F.; Cunha, R.L. Influence of pH on formation and properties of gellan gels. *Carbohydr. Polym.* **2011**, *84*, 662–668. [[CrossRef](#)]
28. Chen, Q.; Tan, L.; Ma, H.; Zhu, J.; Zhang, H. Acid gelation properties of low acyl gellan gum. *Food Sci.* **2017**, *15*, 51–57. [[CrossRef](#)]
29. Hong, J.; Chen, R.; Zeng, X.-A.; Han, Z. Effect of pulsed electric fields assisted acetylation on morphological, structural and functional characteristics of potato starch. *Food Chem.* **2016**, *192*, 15–24. [[CrossRef](#)]
30. Zhao, X.; Wang, Z. A pH-sensitive microemulsion-filled gellan gum hydrogel encapsulated apigenin: Characterization and in vitro release kinetics. *Colloids Surf. B Biointerfaces* **2019**, *178*, 245–252. [[CrossRef](#)]
31. Shirsath, N.R.; Goswami, A.K. Vildagliptin-loaded gellan gum mucoadhesive beads for sustained drug delivery: Design, optimisation and evaluation. *Mater. Technol.* **2021**, *36*, 647–659. [[CrossRef](#)]
32. Lee, H.; Rukmanikrishnan, B.; Lee, J. Rheological, morphological, mechanical, and water-barrier properties of agar/gellan gum/montmorillonite clay composite films. *Int. J. Biol. Macromol.* **2019**, *141*, 538–544. [[CrossRef](#)] [[PubMed](#)]
33. Shao, X.; Sun, H.; Jiang, R.; Yu, Y. Physical and antibacterial properties of corn distarch phosphate/carboxymethyl cellulose composite films containing tea polyphenol. *J. Food Process. Preserv.* **2020**, *44*, 14401. [[CrossRef](#)]
34. Mirani, A.; Goli, M. Production of the eggplant-fiber incorporated cupcake and evaluating its chemical, textural and colorimetric properties over a ten-day storage time. *J. Food Process. Preserv.* **2021**, *45*, e15311. [[CrossRef](#)]
35. Young, P.; Mills, T.; Norton, I. Influence of pH on fluid gels produced from egg and whey protein isolate. *Food Hydrocoll.* **2020**, *111*, 106108. [[CrossRef](#)]
36. Ambebila, E.N.; Santamaría, E.; Maestro, A.; Gutiérrez, J.M.; González, C. Gellan Hydrogels: Preparation, Rheological Characterization and Application in Encapsulation of Curcumin. *Food Biophys.* **2019**, *14*, 154–163. [[CrossRef](#)]
37. Majumdar, R.K.; Saha, A.; Dhar, B.; Maurya, P.K.; Roy, D.; Shitole, S.; Balange, A.K. Effect of garlic extract on physical, oxidative and microbial changes during refrigerated storage of restructured product from Thai pangas (*pangasianodon hypophthalmus*) surimi. *J. Food Sci. Technol.* **2015**, *52*, 7994–8003. [[CrossRef](#)]
38. Boni, F.I.; Prezotti, F.G.; Cury, B.S.F. Gellan gum microspheres crosslinked with trivalent ion: Effect of polymer and crosslinker concentrations on drug release and mucoadhesive properties. *Drug Dev. Ind. Pharm.* **2016**, *42*, 1283–1290. [[CrossRef](#)]

Disclaimer/Publisher’s Note: The statements, opinions and data contained in all publications are solely those of the individual author(s) and contributor(s) and not of MDPI and/or the editor(s). MDPI and/or the editor(s) disclaim responsibility for any injury to people or property resulting from any ideas, methods, instructions or products referred to in the content.